

Characteristics of pore structure and permeability prediction in binary blended pervious concrete

Uma Magesvari Muthaiyan¹ 

¹Rajalakshmi Engineering College, Department of Civil Engineering, 602 105, Chennai, India.

e-mail: umamagesvari.m@rajalakshmi.edu.in

ABSTRACT

This study primarily focuses on analyzing the pore structure characteristics and predicting permeability in binary blended pervious concretes, both with and without fines. The pervious concretes included fly ash, a class 'C' material, as a partial cement replacement (10% and 20%). The aggregates consisted of a mix of coarse aggregates, with sizes ranging from 19–9.5 mm and 9.5–4.75 mm, and fine aggregates substituted a portion of the coarse aggregates at specific levels (5–15%). The area fraction (ϕ_A) and volumetric methodology (ϕ_V) were used for assessing the porosity of the binary blended pervious concrete mixtures. The properties of the pore size were measured through morphological techniques. The Katz-Thompson (K-T) relationship utilized porosity and pore size data from image analysis to predict permeability in pervious concretes. Comparing the two porosity calculation methods, the porosities obtained through image analysis (area fraction) were slightly higher than those obtained through the volumetric technique. The pore characteristics identified through techniques like Two-Point Correlation and granulometry were found to be quite similar. Results indicated a strong agreement between the experimentally determined and predicted permeability values.

Keywords: Binary blended pervious concrete; Pore feature; Porosity; Granulometric function; Permeability.

1. INTRODUCTION

The pore structure attributes of pervious concrete hold vital significance because these factors directly impact the materials' effectiveness and usability. Pervious concrete comprises of cement, coarse aggregate, minimal fine aggregate, additives, and water as its primary components. When these elements come together, they form a solid material with interconnected holes varying from 2 to 8 mm in size, allowing water to permeate rapidly. The estimated void content in pervious concrete typically falls within the range of 15%–35% [1]. Pervious concrete is an essential component of sustainable drainage solutions in urban areas. Through pore structure optimization, it efficiently manages storm water on-site, reducing the strain on traditional storm water infrastructure and mitigating the negative effects of urbanization on natural hydrological systems. Pervious concrete is purposely designed to facilitate water infiltration, allowing groundwater recharge and storm water to pass through it. The material's porosity, influenced by the arrangement of pores, directly determines the rate at which water flows across the pavement surface and permeates into the underlying soil. By carefully designing and maintaining the pore structure, high permeability can be achieved, significantly reducing surface runoff and preventing flooding during heavy rainfall events [2–5].

The way in which pervious concrete samples with varying porosities behave when they fracture is influenced by the interaction between the qualities of their pore structure and the volume fraction of fibers present. By employing stereological and morphological techniques, essential properties related to the pore structure of pervious concrete were discovered [6]. Two methods were employed to assess the porosity of a pervious concrete sample: weighing measurements and X-ray image analysis. Two distinct X-ray imaging setups (2D and 3D) were utilized to capture cross-sectional planar visuals of a cylindrical pervious concrete specimen. Remarkably, the outcomes obtained from weight measurements and the porosity estimation via the 2D X-ray analysis exhibited striking similarities [7]. The unique features of pervious concrete's pore system, which may be evaluated by computing the mean pore size utilizing a specialized linear path function, possess an impact on the behavior of the material in terms of compressive strength.

This unique linear path function has been tested using image analysis and is designed specifically for pervious concrete [8]. The pore distribution characteristics in pervious concrete are examined under various

proportioning techniques involving different paste content, aggregate size and compacting effects. These features of the pore structure are determined through volumetric analysis and image analysis. Subsequently, the obtained characteristics are utilized in the Katz-Thompson equation to predict permeability [9–12]. Porosity is measured using mathematical morphology and stereology methods to extract distinctive pore features. Interestingly, it has been found that the typical pore diameters obtained through these various approaches show a strong correlation. Research has demonstrated that meticulous manipulation of aggregate grading and synthesis can enhance the connectivity within the pore structure, effectively boosting the permeability of pervious concrete. This improvement occurs through methods that focus on enhancing pore connectivity rather than merely increasing pore diameters or overall porosity [13–16].

As several kinds of techniques, both direct and indirect, were utilised to reveal the microstructures, permeability assessments were performed up using the Katz-Thompson model, pore connectivity simulation, and computational fluid dynamics. Several techniques were utilised for assessing the pore structure's features. However, observed permeability, which is based on pore structures acquired from various methods, reveals significant variations with respect to the pore size ranges that have been identified through the experiments [17]. Establishing and validating the suitability of the (K-T) model to concrete materials, pore structure parameters were analysed using mercury intrusion porosimetry. The Klinkenberg effect corrections were used to evaluate the permeability of 48 concrete samples, and gas permeability testing was conducted. The experimental and predicted permeabilities were compared in order to calculate constant. The study confirmed that the K-T model can be applied to concrete and found a variable K-T constant that strongly correlates with the water/binder ratio [18]. A 2-D, 3-parts finite element representation of a microstructure model is used to forecast concrete permeability using actual aggregate morphologies and digital photography. Higher water-to-cement ratios increase permeability, according to the Model, which underwent validation using experimental data with a 1.73% relative error. It demonstrates an inverse link between permeability and aggregate content, with rounder aggregates increasing permeability and larger aggregates decreasing it by examining variables such as aggregate content, features, position, and ITZ thickness. Segregated concrete is less permeable than uniformly dispersed concrete, and higher ITZ thickness is associated with higher permeability. The Model provides a thorough understanding of the dynamics of concrete permeability, which is essential for optimizing concrete mixtures for a range of applications [19].

As a result of its large pores, pervious concrete—valued for its environmentally beneficial qualities—has clogging difficulties. This study examined the distributions of pore sizes and permeability reduction in pervious concrete. It was discovered that thickness has a minor effect on permeability but a major impact on clogging behaviors. The anti-clogging performance was found to be significantly predicted by clogging sand sizes and featured pore size [20]. The microstructure of Engineered Cementitious Composite (ECC) paste was simulated using the HYMOSTRUC model. The GEM theory was applied to evaluate the permeability. Porosity and permeability of the Interfacial Transition Zone were evaluated, as well as other parameters obtained from mix proportions. Tests on water permeability confirmed that adding PVA fibres to ECC resulted in a slight decrease in its water permeability coefficient. There was a discrepancy in the expected and actual permeability values, as evidenced by the significant 27.1% deviation [21]. The experimental study examined how variations in mix variables influenced functional performance of pervious concrete. The contributions of each individual variable to permeability were determined by statistical analysis. Pore tortuosity was addressed by hydraulic conductivity, which was measured and predicted by the Kozney-Carman model using a modified K-C model. The focal point was average pore size obtained by ancestral path function [22]. Attempts have made to recreate several numerical models using pore structure data acquired through image analysis, MATLAB code was employed [23].

A novel permeability prediction model, named K-T Modified, has been introduced. This Model leverages the anticipated the mean cement paste thickness and the average size of aggregates. Through comparative analysis, it has demonstrated a robust correlation by predicting permeability values [24]. This study aims to examine and describe the pore structure of dual-component pervious concrete mixtures with and without fines, utilizing cement concentrations of 250 kg/m³ and 300 kg/m³. To achieve this, a partial replacement of cement was carried out using 10% and 20% class C-fly ash, respectively. The concrete blends were comprised of a 60:40 proportion of coarse particles, spanning from 19 to 9.5 mm and 9.5 to 4.75 mm in size. Moreover, an industrially available plasticizer was incorporated into the pervious concrete formulations, while fine aggregates were introduced to substitute 5% to 15% of the coarse aggregates. Permeability predictions for the pervious concretes were made using image analysis methods and the Katz-Thompson relationship. Permeability predictions for the pervious concretes were made using image analysis methods for determining the pore features and used to develop Katz-Thompson and Katz-Thompson Modified Model. These predictions were compared with experimental results obtained under identical conditions.

2. MATERIALS

2.1. Material and mix proportioning

For proportioning pervious concrete mixes, cement contents of 250 and 300 kg/m³ were considered, both with a specific gravity of 3.15. The cement sets in 35 minutes initially and 150 minutes finally, with a standard consistency of 33.5%. Its 1 mm soundness indicates a restricted expansion after setting. These cement content ranges cover the potential applications of permeable base coarse materials, such as sub-base and base coarse. The control mixes of pervious concrete were designed using these cement contents as a basis. The control mixes exclusively employed coarse aggregate. Fly ash sourced from a thermal power plant located in Neyveli, Tamil Nadu, India, possessing a specific gravity of 2.45, was introduced into each blend. It has a standard consistency of 35% and requires 40 minutes to set initially and 250 minutes to set completely. When the soundness is zero millimeter, stability is indicated. The fineness is 340. Furthermore, the lime's reactivity of 7.0 MPa indicates that it has the potential to gain strength. The utilized fine aggregate exhibited a specific gravity of 2.62, a fineness modulus of 2.86, a water absorption rate of 1% and adhered to the standards of IS:383-1978 zone II.

Each control mix included choices for 10 and 20% (by weight) fly ash replacement of cement. Additionally, 5%, 10%, and 15% (by weight) of the coarse material was replaced with fine aggregate. The coarse aggregates used had a specific gravity of 2.71 with an abrasion value of 19%, water absorption at 0.1%, a crushing value of 14%, impact value of 16% and were made up of 60% of the total content in the 19 mm to 9.5 mm size range and 40% in the 9.5 mm to 4.75 mm size range. The pervious concrete mixes incorporated the commercially accessible plasticizer CONPLAST-P211, following the approved dosage of 0.8% based on the cement weight. In all analyzed mixtures investigated, a consistent water-cement (w/c) ratio of 0.3 was upheld.

As there was no equivalent Indian code available expressly for pervious concrete, the mix designs were carried out in accordance with ACI 522 R-10 [1]. Six control mixes without fines comprising two without fly ash, two with 10% fly ash substitution, and two with 20% fly ash substitution were proportioned. Additionally, 12 mix of fly ash-based six for the 10 and 20% substitution levels were created, along with 6 mixes with fine aggregate contents varies from 5 to 15%. These mixtures were used to cast specimens, which allowed to examine their permeability, void, and pore feature characteristics.

3. EXPERIMENTAL PROGRAM

3.1. Permeability

Cylindrical specimens measuring 90 mm in dia and 150 mm in height were fabricated as shown in Figure 1 and subsequently subjected to testing following a standard 28-day curing period. Due to the lack of an Indian comparable standard, the falling head permeability procedure was conceptualized and documented by Narayanan Neithalath and his associates. They developed a dedicated experimental arrangement tailored to measure the permeability of pervious concrete specimens through this approach [25]. ACI 522R-10 [1] has also established the aforementioned process as standard procedure.

3.2. Fresh state porosity

The calculation of void content in fresh state pervious blended concretes is carried out in accordance with ASTM C 1688/C 1688 M-13 standards. It is used to measure the indirect passing category to pervious concrete. Void presents in pervious concrete must be more than 15%. If satisfied in the fresh void, volumetric porosity also lies above the same. A cylindrical container of 7-lit capacity is placed onto a level and stable surface that is both flat and even. Prior to introducing pervious concrete, the interior of the cylinder is dampened and subsequently dried. Any residual moisture within the container is removed. The cylinder is then filled using two layers of nearly uniform thickness of pervious concrete. In a repetitive manner, the proctor hammer is dropped vertically from a distance of 305 mm a total of twenty times for each layer. In order to ensure consistent and uniform compaction across the whole surface area of the pervious concrete, the impacts are evenly distributed. Prior to compacting the final layer, the cylinder is filled until it overflows. The upper surface of the concrete is levelled off after the consolidation process is completed. Measure the weight of cylinder with and without binary blended pervious concrete to evaluate the fresh Voids present in the mixes.

3.3. Volumetric porosity at hardened state

Cylindrical specimens of 90 mm in dia and 150 mm in height, were fabricated and applying the standard 28-day curing procedure. Subsequent to the curing phase, the volumetric porosity of the pervious concrete specimens



Figure 1: Experimental setup of permeability testing.

were assessed in accordance with the directives outlined in ASTM C 1754/C 1754M-12. The weight difference between a sample that was oven-dried and then immersed in water was used to determine the porosity (ϕ_v).

3.4. Binary blended pervious concrete two-dimensional image acquiring and processing

Using image analysis methods on two-dimensional images, the pore structure feature of pervious concrete mixtures were identified. For image processing, 50 mm thick slices of 90 mm in diameter by 150 mm in length cylindrical specimens of pervious concrete were cut into. To provide smooth surfaces suited for image acquisition, the cut surfaces were meticulously ground. Six to eight suitable faces were used for image capture for each combo. These faces were scanned with a flatbed scanner over a clear plastic film to create grayscale images. 'Image J', was used to process the images. The further image processing procedures were carried out: The porous and solid phases were successfully separated by cropping the grayscale images into circular images with a diameter of 570 pixels before converting them into binary images using a thresholding method. For all of the photos utilised in this investigation, the upper limit of the relevant pore phase grey level was set within the range of 120 to 130. To get rid of any noise or artefacts, the binary pictures underwent further cleaning. The pore structure features were recovered from the processed circular images using 400×400 pixels square pictures as shown in Figure 2. This process was based on the previously published work [13, 14].

3.5. Permeability prediction equation for pervious concrete

The Katz-Thompson (KT) relationship, extensively acknowledged for cross-property correlations in permeability, is well-documented in references [19, 26, 27]. Originally proposed by KT, the constant (ckt) was recommended to be $1/226$. Over time, the KT relation has demonstrated its efficacy in offering reliable estimates for the permeability of sandstones. The assessment of porosity and permeability in sandstone samples was conducted through the thin section analysis technique.

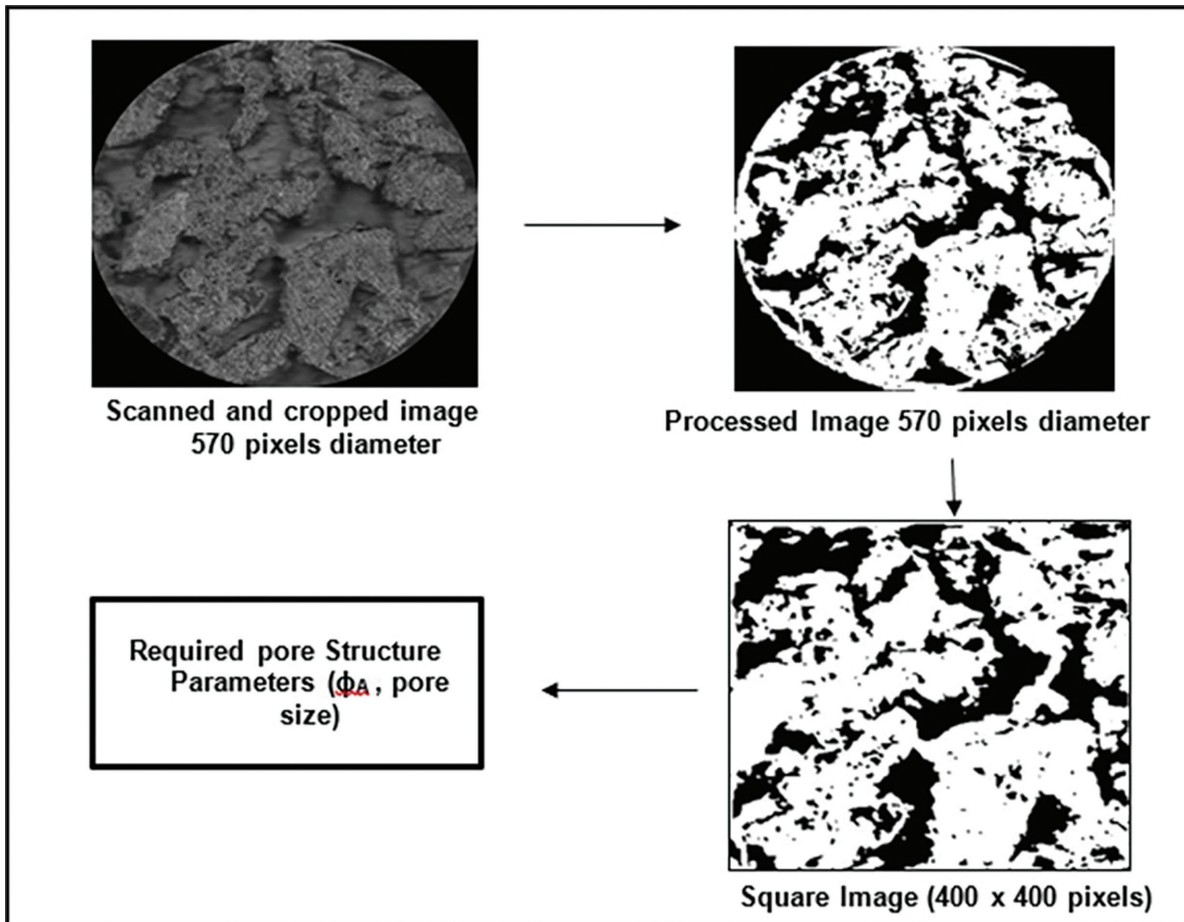


Figure 2: Illustrates the steps involved in acquiring the pore structure features.

Image analysis yielded results that closely matched those obtained through the traditional core plug methods. The range of porosity values varies between 15 to 27% [28].

Precision of permeability calculations in pervious concrete, the Katz-Thompson equation incorporates a hydraulic connectivity factor. This factor combines three crucial elements influencing permeability: open porosity, pore connectivity and pore size [9, 11, 13].

A novel model (K-T Modified) was introduced by Wang *et al.* 2020 [24] that relies on the anticipated mean thickness of cement paste and the average size of aggregates. The permeability prediction model utilized have a strong correlation by comparing the predicted permeability values with assessed previously established by Neithalath *et al.*

Katz-Thompson Model and Modified K-T Model have been used to predict the permeability of pervious concrete.

Katz-Thompson [19] utilized percolation theory to establish a correlation between air permeability and the critical pore diameter of sedimentary rock. They suggested equation (1) as a result of their research.

$$k = \frac{1}{226} d_c^2 \frac{\sigma}{\sigma_0} \quad (1)$$

Symbols are defined as follows: k represents intrinsic permeability in square meters, d_c denotes the critical pore diameter in meters, σ represents bulk conductivity in (S/m), and σ_0 stands for pore solution conductivity in (S/m). The validity of the Katz-Thompson equation has been examined in studies focusing on cementitious materials, particularly through water permeability assessments. CHRISTENSEN *et al.* [29] observed that the relationship holds true based on their findings.

$$\frac{\sigma}{\sigma_0} = \frac{d_{max}^e}{d_c} \eta S(d_{max}^e) \quad (2)$$

Additionally, the formation factor (σ/σ_0) was determined from the pore parameters using Equation (2) [30]. In this equation, d_{max}^e is calculated as 0.34 times the critical pore diameter (d_c). The critical pore diameter (d_c) is a parameter in the formula, while η represents the total porosity expressed as a percentage. $S(d_{max}^e)$ corresponds to the fractional volume of pores larger than d_{max}^e .

The conversion from 'intrinsic' permeability (k , in m^2) to conventional permeability (K , in m/s) is achieved by employing the formula proposed by CHRISTENSEN *et al.* [29] in 1996. This enables a comparison between the predicted permeability values and the actual experimental values. This transformation allows for a direct comparison between the two permeability measurements.

Wang *et al.* [24] in 2020 introduced a novel model (K-T Modified) for the permeability prediction determination as given in equation 3.

$$k = 0.412 \cdot e^{Pt} \cdot \left(\frac{da}{t} \right)^{n1.812} \quad (3)$$

K = permeability, Pt = total porosity, t = Mean thickness of the cement paste and da = average size of aggregate.

3.6. Area fraction of pores (ϕ_A)

The image analysis technique is used to estimate the proportion of pore area. This process involves utilizing specific analytical tools within the image processing software to distinguish individual pores in the threshold image. The pore area proportion is subsequently computed by summing and dividing the combined area of all these individual pores by the total area of the entire image.

3.7. Pore size

Pervious concrete contains a well-defined pore structure, and the assessment of pore diameters is conducted using both stereological and mathematical morphological methods. Stereology involves numerically describing the geometrical and statistical characteristics of pore distribution. On the other hand, mathematical morphology focuses on analyzing how images change under specific transformations [31, 32].

In this study, two specific morphological measures, namely the two-point correlation (TPC) function (d_{TPC}) and granulometry (d_{crit}), are employed to characterize the pore sizes in pervious cement and fly ash concretes. These morphology-based approaches enable precise measurement and analysis of the pore sizes within the materials under investigation. The Two-Point Correlation (TPC) function, a morphological approach, is employed for the analysis of a distinct phase within a two-phase material. This method provides valuable insights into parameters such as the pore area fraction, featured pore diameters, and a defined pore surface area.

Pore diameter (d_{TPC}) is given in Equation 4.

$$d_{TPC} = \frac{l_{TPC}}{1 - \phi_A} \quad (4)$$

Pore diameter of a mix for Pervious blended pervious concrete is shown in Figure 3 using Two-point Correlation Method.

The arrangement of different sizes of features within a 2-D image is elucidated through the granulometric distribution function, which relies on a morphological opening-based distribution approach. This involves plotting the pore area fraction against the size of the structuring element following an opening operation. Circular structuring elements are utilized to compute the granulometric density functions $G(k)$. The Critical pore size (d_{crit}) represents the perimeter of the circular structuring element that aligns with the peak in $G(k)$. Pore Size of a mix for Pervious blended pervious concrete is shown in Figure 4 using granulometric function.

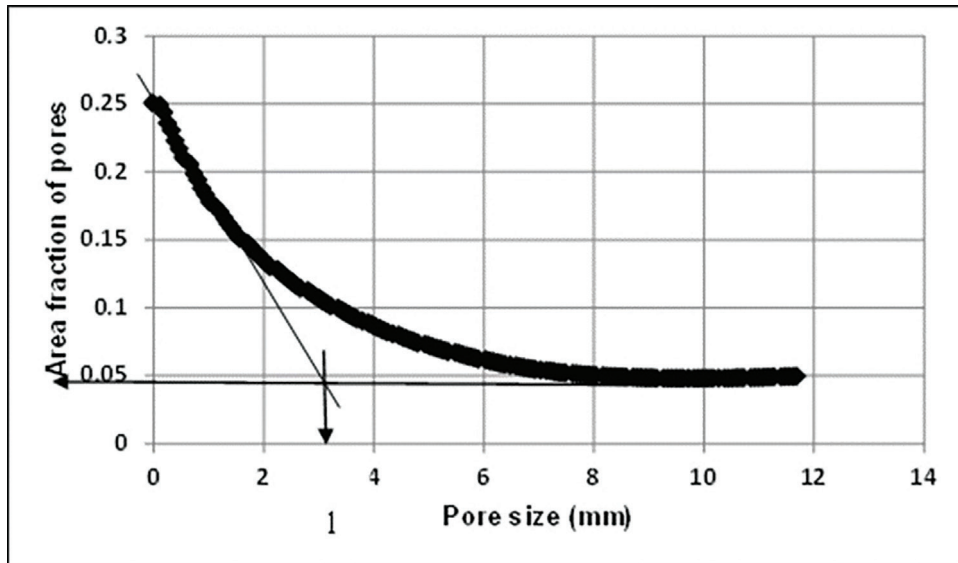


Figure 3: Pore size Vs area fraction of pores.

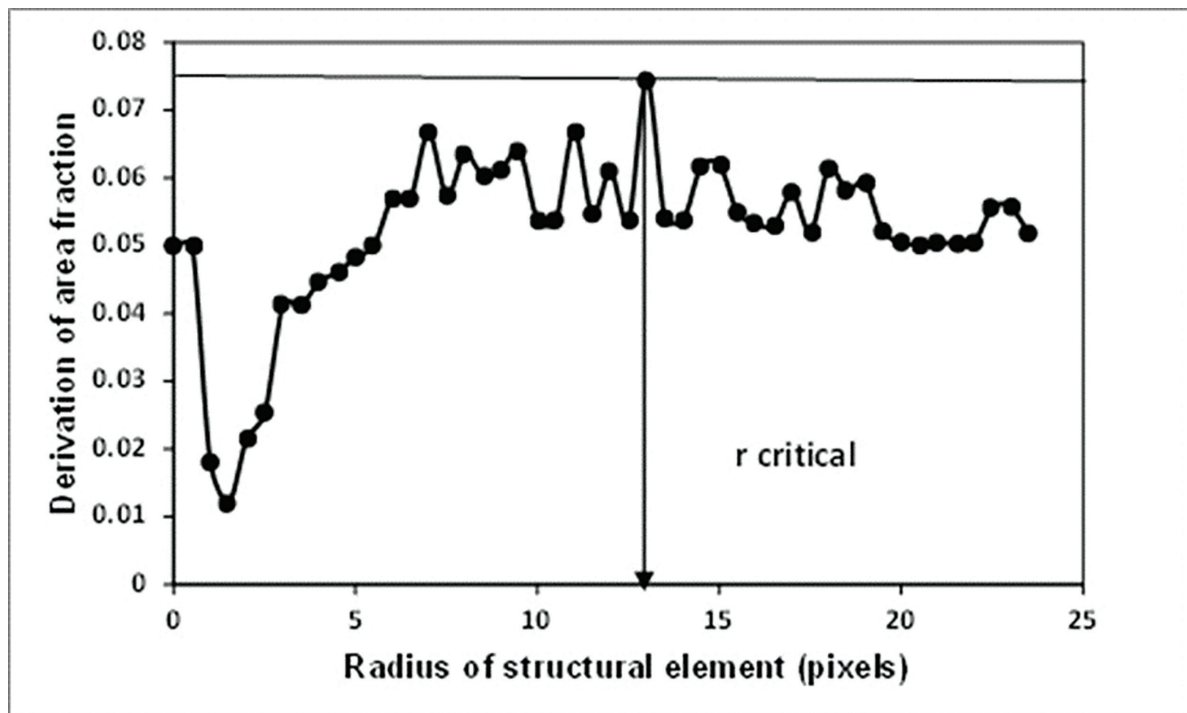


Figure 4: Granulometric density function of a blended pervious concrete.

4. RESULTS AND DISCUSSION

4.1. Voids present in fresh blended pervious concrete

Variation of fresh void as shown in Figures 5 and 6 in pervious binary blended cement concrete, both with and without the inclusion of fine and fly ash substitutes at levels of 10% and 20% in relation to the cement content. The fresh voids percentage spans from 19.17% to 24.87% in the absence of fine additives for mixes involving both binary blended pervious concrete and regular mixes. When fly ash is not replaced, the inclusion of fines results in percentages ranging from 17.45% to 22.04%. However, in cases where fly ash is substituted in binary blended pervious concrete, the range narrows to 14.41% to 19.86%. With an augmentation in binder content,

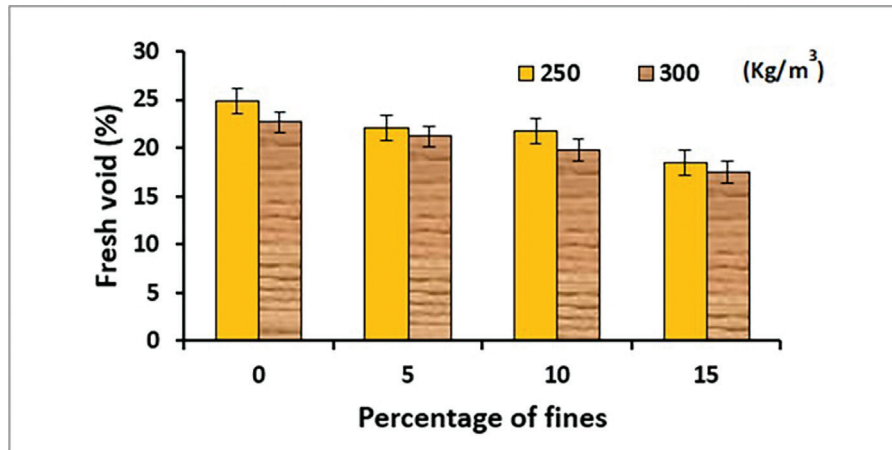


Figure 5: Fresh voids of pervious concrete with fines percentage.

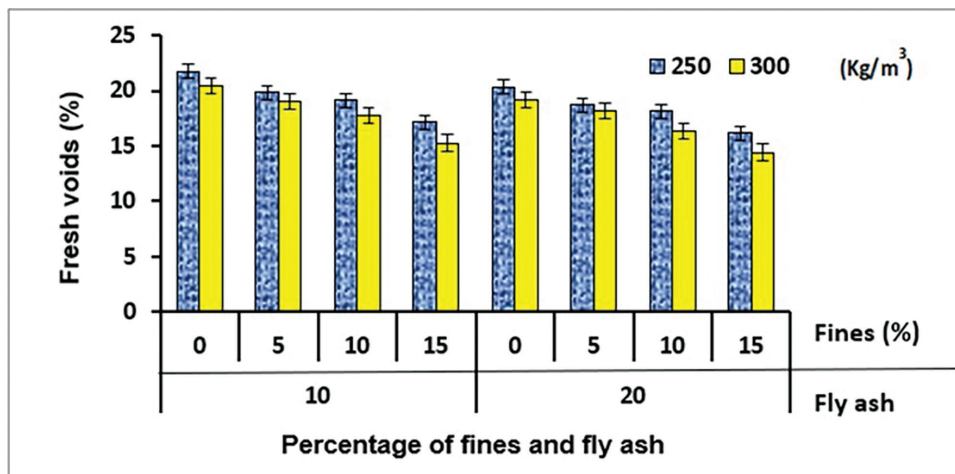


Figure 6: Fresh voids of Binary blended pervious concrete and different fines percentage.

there is a gradual reduction in the proportion of overall voids during the fresh state, and this trend persists with the increase in fine content.

4.2. Pore area and volumetric porosity in hardened binary blended pervious concrete

Processed image for cement content and fly ash replacement for various fine aggregates are shown in Figures 7 and 8. Figures 9 and 10 depict the variation between the volumetric porosities of binary blended pervious concretes and the pore area fractions derived from image analysis of planar sections. By considering the cement content 250 kg/m³ and its fly ash replacements without fines, A decrease in volumetric porosity is observed and the same trend is followed in the area fraction of pores, which is slightly higher than volumetric porosity. Additionally, the area fraction of pores has shown that the overall void content (volumetric porosity) decreased as a result of the addition of fines (5% to 15%) and the replacement of fly ash for cement. The above behaviour is similar in case of cement content 300 kg/m³ and its replacements of fly ash with and without fines. The volumetric porosity is almost equal to the pore area fraction found from 2-D image. Pervious cement concrete exhibits a volumetric porosity ranging from 18.68% to 27.37%, regardless of the presence of fines. The corresponding pore area fraction, as determined through image analysis, simultaneously varies between 20.91% and 27.7%. In the case of fly ash pervious concrete 10 and 20%, the volumetric porosity varies from 18.19% to 26.47% and 16.82% to 23.55%, whether or not fines are included. For fly ash contents of 10% and 20%, respectively, the corresponding pore area fraction determined by image analysis ranges from 19.6% to 26.6% and 17.2% to 24.1%. Notably, there exists a mere 6% disparity between the volumetric porosity and pore area fraction. According to

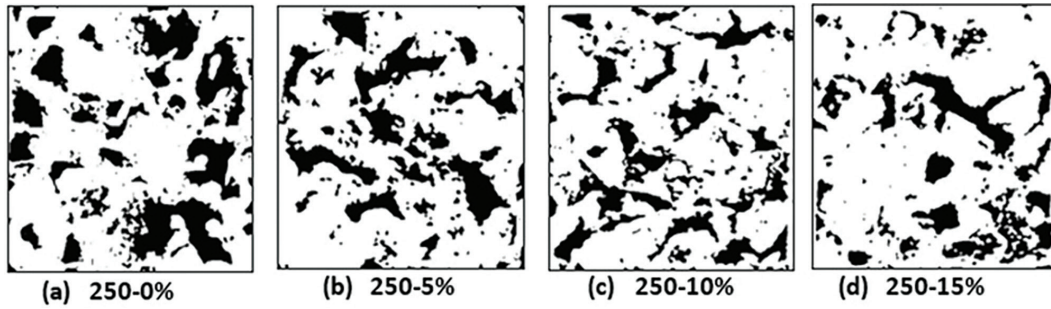


Figure 7: Image analysis of pervious cement concrete 250 kg/m³ pore characteristics for different fines contents.

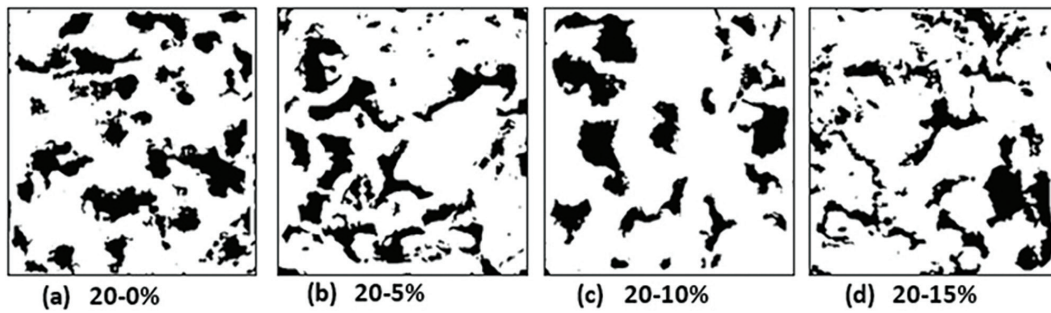


Figure 8: Image analysis of binary blended pervious concrete (20% fly ash) -pore characteristics for different fines contents.

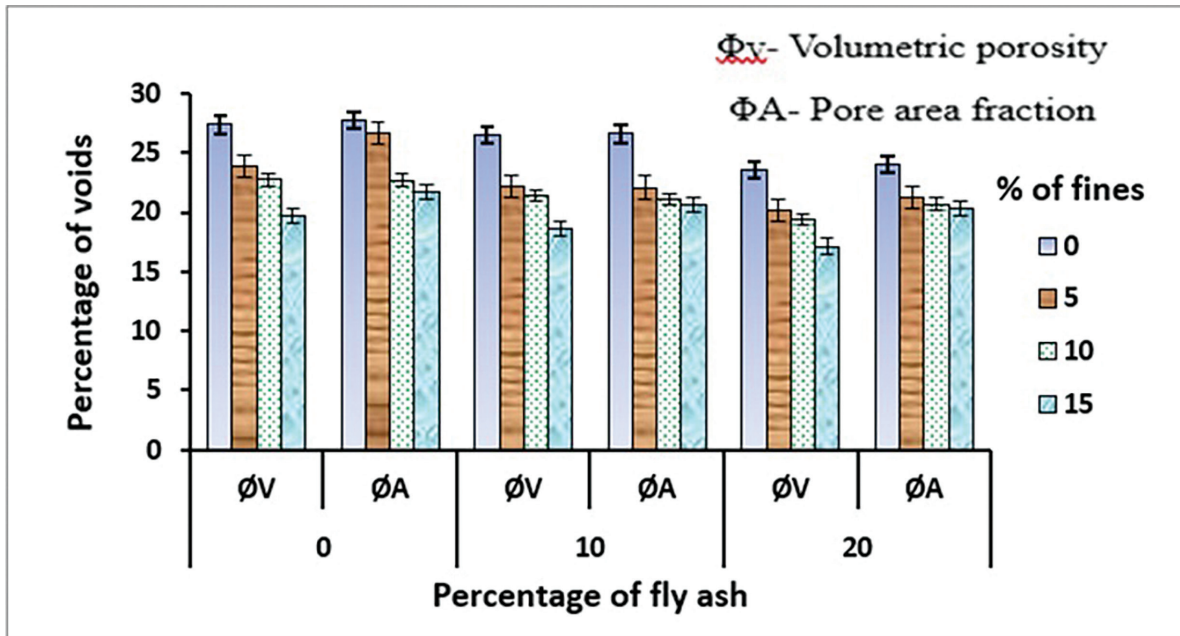


Figure 9: Percentage of void vs percentage of fine aggregate and fly ash replacement for Binder content 250 kg/m³.

ACI 522-R10 guidelines, the void content values, spanning from 16.82% to 26.47%, accounting for the incorporation of fly ash and the introduction of fine aggregate, align with the established void content range standards observed across all the mixtures.

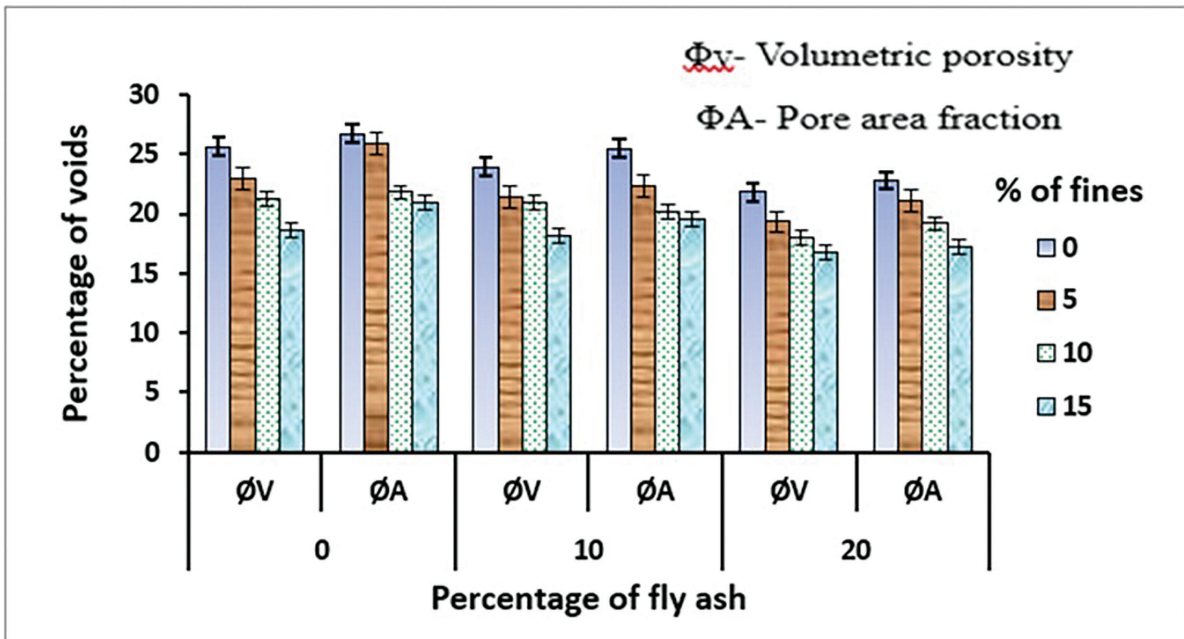


Figure 10: Percentage of void vs percentage of fine aggregate and fly ash replacement for Binder content 300 kg/m³.

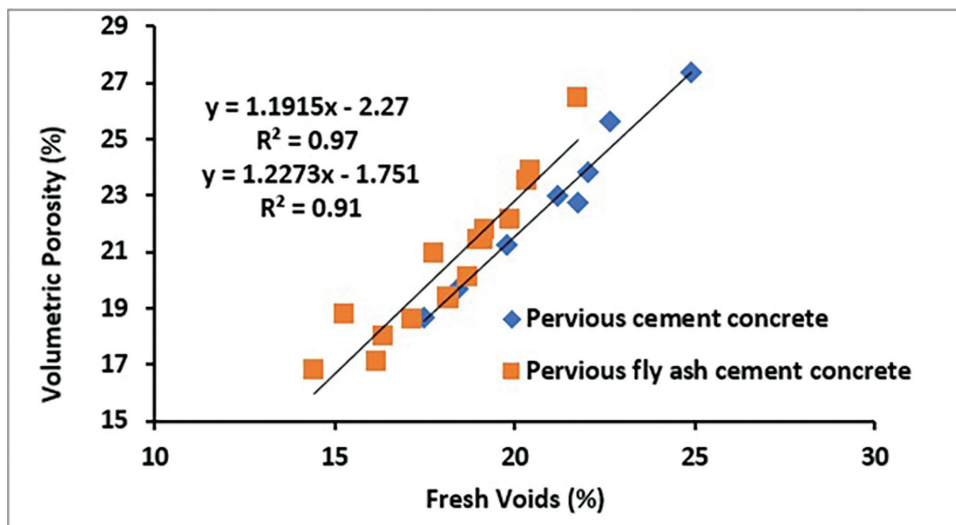


Figure 11: Relation between Fresh voids and volumetric porosity for pervious concretes.

4.3. Relation between fresh void and volumetric porosity

Variation of Fresh voids and volumetric porosity for pervious concrete and binary blended pervious concrete illustrated in Figure 11. Pervious concrete should have more than 15% voids; for measuring indirect characteristics, fresh void is measured. The correlation between fresh voids and volumetric porosity in pervious concrete and binary blended pervious concrete is characterized by regression coefficients of 0.97 and 0.91, signifying a robust fit in both cases.

4.4. Pore size from two-point correlation (d_{TPC})

The variation in pore size based on TPC is depicted for a binder content of 250 kg/m³, and partial replacement levels of fly ash at 10% and 20%, both with and without fines as illustrated in Figure 12. Pore size of pervious cement concretes without fines is 5.177 mm, which gets reduced for various fly ash replacements levels. It is

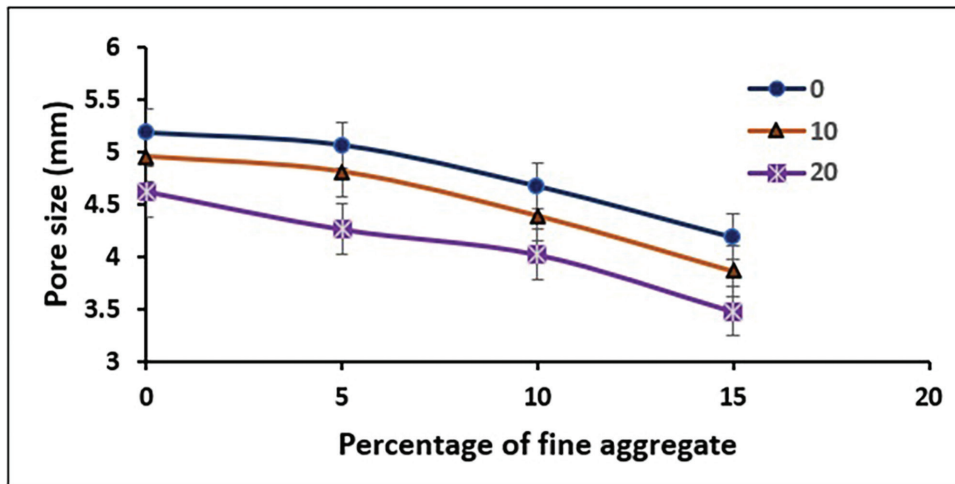


Figure 12: Pore size (d_{TPC}) with fine aggregate percentage for various fly ash replacement for the Binder content 250 kg/m³.

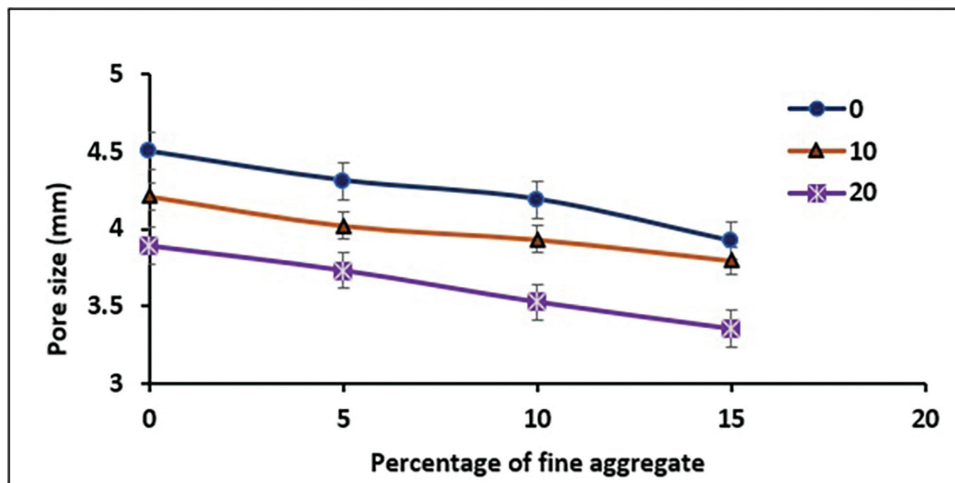


Figure 13: Pore size (d_{TPC}) with fine aggregate percentage for various fly ash replacement for the Binder content 300 kg/m³.

seen that due to addition of fines (5% to 15% and fly ash replacements with fine aggregates, in pervious concrete it has decreased the in-pore size. The range of pore size varies between 5.177 to 3.480 mm. Considering every conceivable combination of mixtures, the trend remains consistent for pervious concretes with binder contents of 300 kg/m³, varying degrees of fly ash replacement, and both with and without fines. This pattern mirrors that observed in pervious concretes with binder contents of 250 kg/m³, as depicted in Figure 13. The pore size varies from 4.501 to 3.351 mm.

4.5. Pore size from granulometric distribution (d crit)

The variation in pore size based on granulometry is depicted for a binder content of 250 kg/m³, and partial replacement levels of fly ash at 10% and 20%, both with and without fines as illustrated in Figure 14. Pore size of pervious cement concretes has been reduced for various fly ash replacement levels. It is seen that due to addition of fines (5% to 15% and fly ash replacements, with fine aggregates, in pervious concretes have decreased the pore size. The range of pore size varies between 5.611 to 3.922 mm. Considering all combination of mixes considered. Both with and without fines, pervious concretes featuring a binder content of 300 kg/m³ and various degrees of fly ash replacement display a pattern identical to that observed in pervious concretes with a binder content of 250 kg/m³, as illustrated in Figure 15. However, the pore size varies between 4.964 to 3.572 mm. It is seen that d_{crit} (granulometry) values are slightly higher than d_{TPC} obtained from two-point correlation method, by the same image. The percolation threshold in the mixture is associated to the pore size.

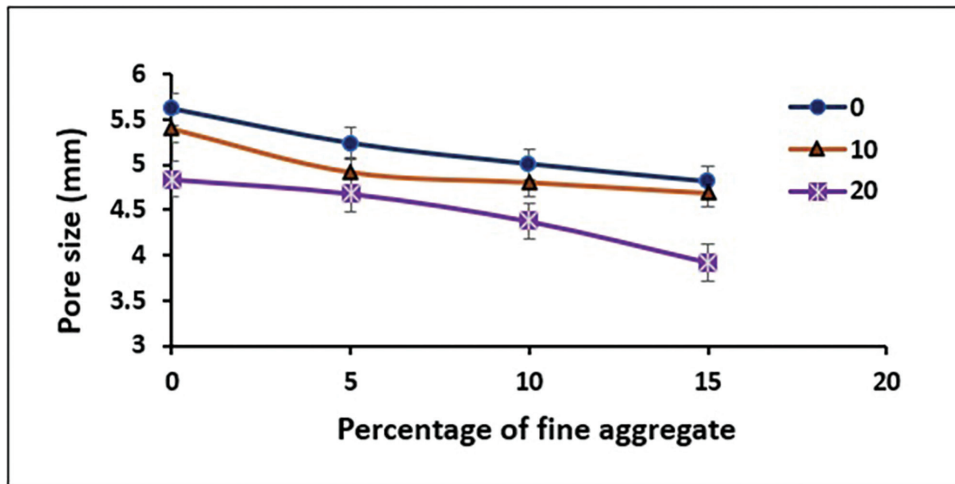


Figure 14: Pore size (granulometry) vs fine aggregate percentage for fly ash replacements for the binder content 250 kg/m³.

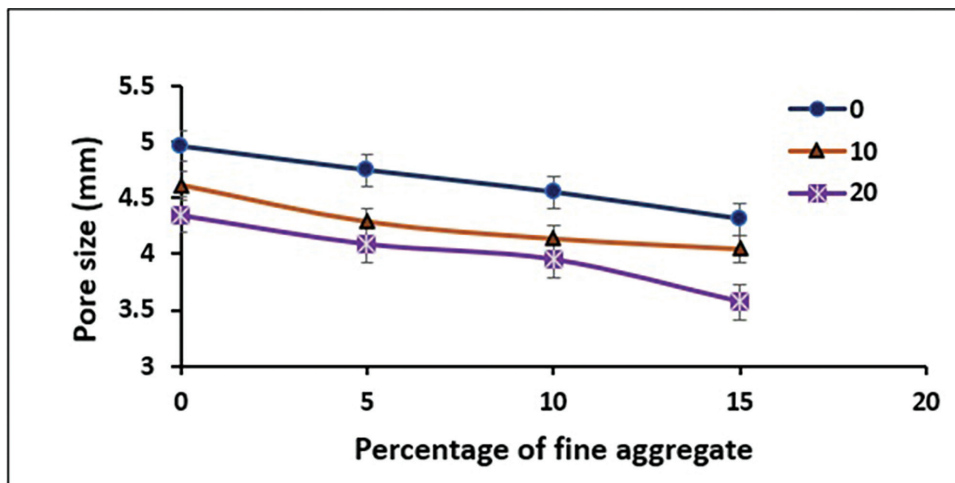


Figure 15: Pore size (granulometry) vs fine aggregate percentage for fly ash replacements for the binder content 300 kg/m³.

4.6. Permeability

The permeability of fines-free pervious cement concretes decreases as the cement content increases, varying from 1.149 to 0.889 cm/s. Across all levels of fly ash replacement in pervious fly ash-cement concretes, exhibiting a permeability range of 1.093 to 0.751 cm/s, a consistent trend is observed. The permeability varies between 0.931 and 0.354 cm/s when accounting for various degrees of fine aggregate replacement. Overall, there is an average reduction of about 13.28% in permeability, considering both the presence and absence of fines (Figure 16).

4.7. Permeability prediction using pore structure features

The pore feature are determined using image analysis. Further, it is used to determine (σ/σ_0) which is presented in Equation (2). Sample calculation of (σ/σ_0) for cement content 250kg/m³ with zero fines, corresponding values of $d^*_{max} = 0.34d_c$, d_c = critical pore diameter, $\eta = 27.7(\%)$, $S(d^*_{max}) = 0.98$ and (σ/σ_0) is calculated as 0.092. The values of (σ/σ_0) for all the mixes are presented in Table 1. Pore size and (σ/σ_0) are used to obtain the permeability prediction for all the cement fly-ash pervious concrete using Equation (1).

The experimentally measured permeability using falling head method and the predicted permeability determined using Katz-Thompson (K-T) relationship, using the measured pore size from TPC and granulometry are shown in Figures 17 and 18.

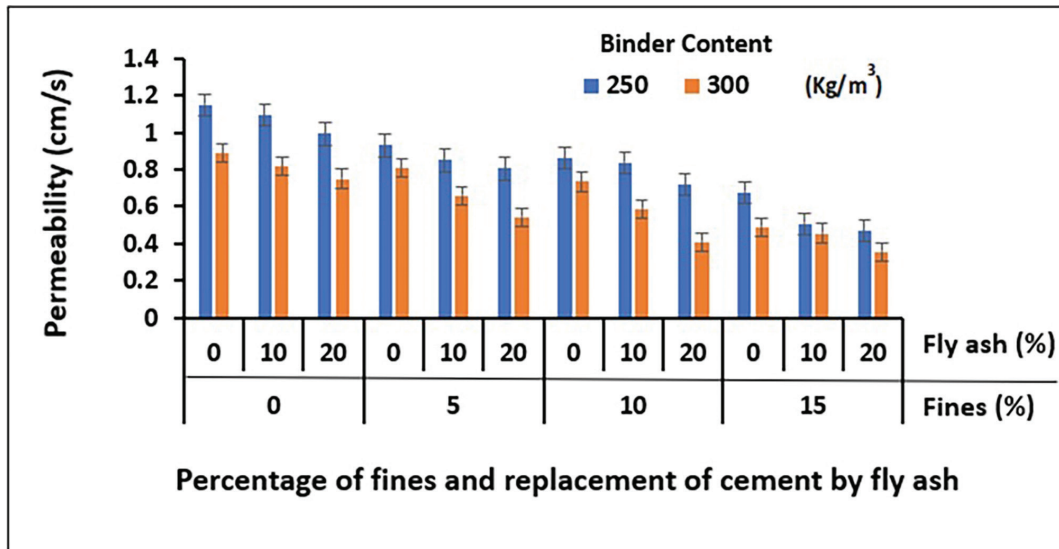


Figure 16: Permeability for different binary blended pervious concrete.

Table 1: (σ/σ_c) for pervious cement – fly ash mixes.

CEMENT CONTENT	PERCENTAGE OF FINE	REPLACEMENT OF FLY ASH		
		0	10	20
250	0	0.092	0.089	0.080
	5	0.089	0.072	0.072
	10	0.073	0.069	0.069
	15	0.069	0.067	0.068
300	0	0.088	0.086	0.077
	5	0.087	0.075	0.071
	10	0.083	0.071	0.062
	15	0.074	0.066	0.057

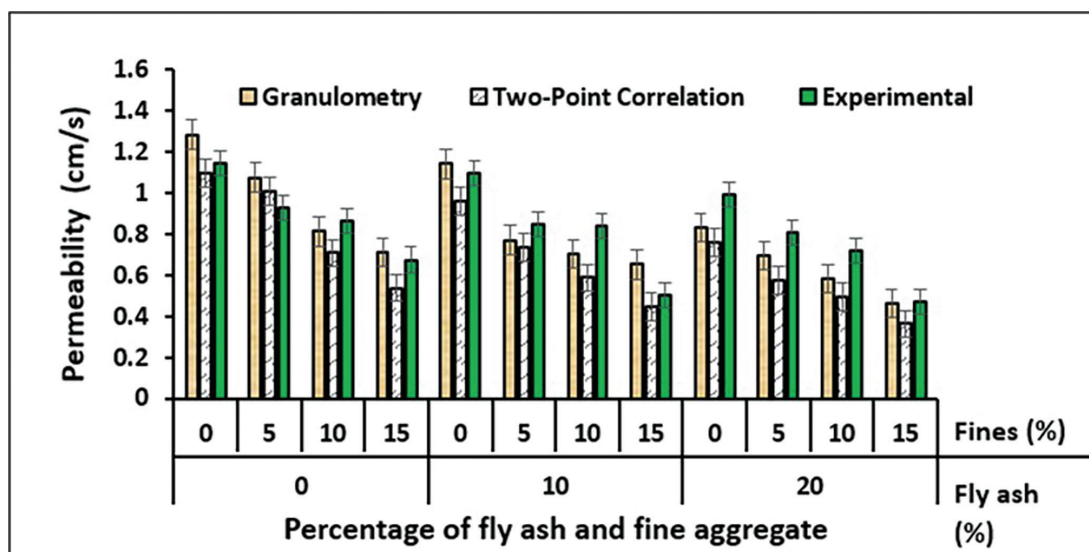


Figure 17: Comparison of permeability (predicated vs experimental) for binary blended pervious concrete for binder content of 250 kg/m³.

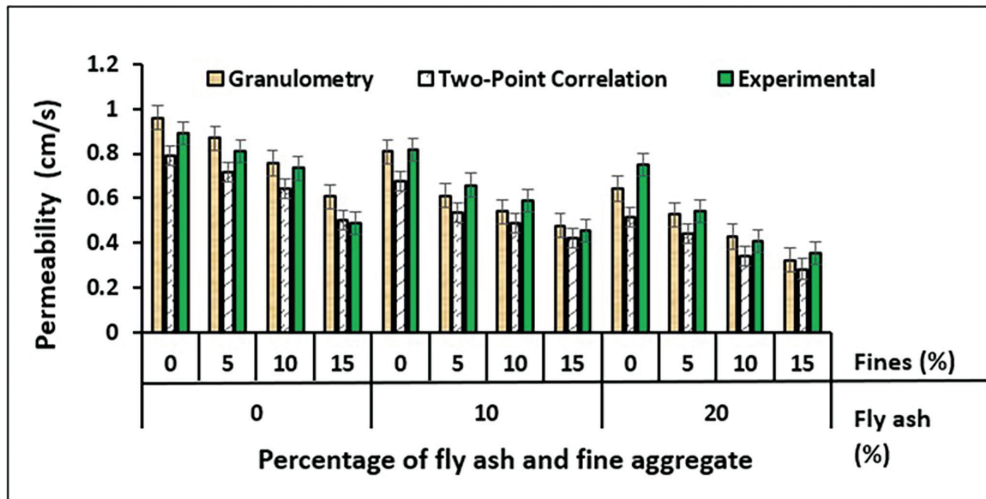


Figure 18: Comparison of permeability (predicated vs experimental) for binary blended pervious concrete for binder content of 300 kg/m³.

The permeability of pervious cement concretes without fines decreases with the replacement of fly ash. A similar trend is observed in pervious cement concretes with fines for all the considerable degree of fly ash substitution. However, the permeability of binary blended pervious concretes is generally lower than that of pervious cement concretes. This pattern is also evident in the predicted permeability using pore sizes obtained from both the TPC and granulometry methods. Both including and excluding fines, the permeability of binary blended pervious concrete spans from 1.149 to 0.354 cm/s. TPC approach produced predicted permeability values for pervious concrete with an average of 0.92. This shows a mean inaccuracy of about 8%, within the commonly accepted bounds of less than 10%. On the other hand, the average projected value by the granulometry approach was 1.09. The granulometry approach’s higher anticipated values align with predictions, and the average permeability prediction error is about 9%, which is within acceptable bounds and similar to the TPC method. The TPC-predicted permeability values with an average of 0.83, for binary blended pervious concrete. Considering both replacement levels, the average error is 12.5%, marginally higher. On the other hand, the granulometry technique predicted values with a mean of 1.05 for binary blended pervious concretes. Considering both replacement levels, the granulometric method’s average inaccuracy in anticipated values is 5.5%. In general, the granulometric approach regularly performs better than the TPC approach.

4.8. Permeability predictions using cement paste thickness

The experimentally measured permeability using falling head method and the predicted permeability determined using Katz-Thompson modified (K-T-M relationship, using the estimated cement paste thickness using image analysis illustrated in Figure 19. The permeability of binary blended pervious concretes is generally lower than that of pervious cement concretes. The same pattern is also evident in the predicted permeability using average aggregate thickness and cement paste thickness obtained from Image analysis method.

4.9. Permeability prediction models for pervious concrete

Remarkably, the predictions align quite closely with the experimental data employed in this work. Figure 20 depicts the correlation between permeability obtained from the experiment vs predicted permeability by the Katz-Thompson Model and the Katz-Thompson modified Model. Correlation for cement pervious concrete and fly ash cement pervious concrete for both Katz-Thompson using Granulometry method by Image analysis given as K-T(G), Katz-Thompson using two-point correlation method by Image analysis given as K-T(TTP) and Modified Katz-Thompson model using paste thickness by image analysis K-T-M was determined. Katz Thomson modified Model showing a strong agreement with the regression coefficient of 0.97 and 0.96. Cement pervious concrete represents higher regression coefficient for all the models, whereas binary blended pervious concrete shows slightly lower regression coefficient than cement pervious concrete.

4.10. Application based on permeability

The Federal Highway Administration (FHA) in the United States propose a minimum permeability of 300 meters per day (equivalent to 1000 feet per day or 0.347 cm/s). Furthermore, the selection of materials is

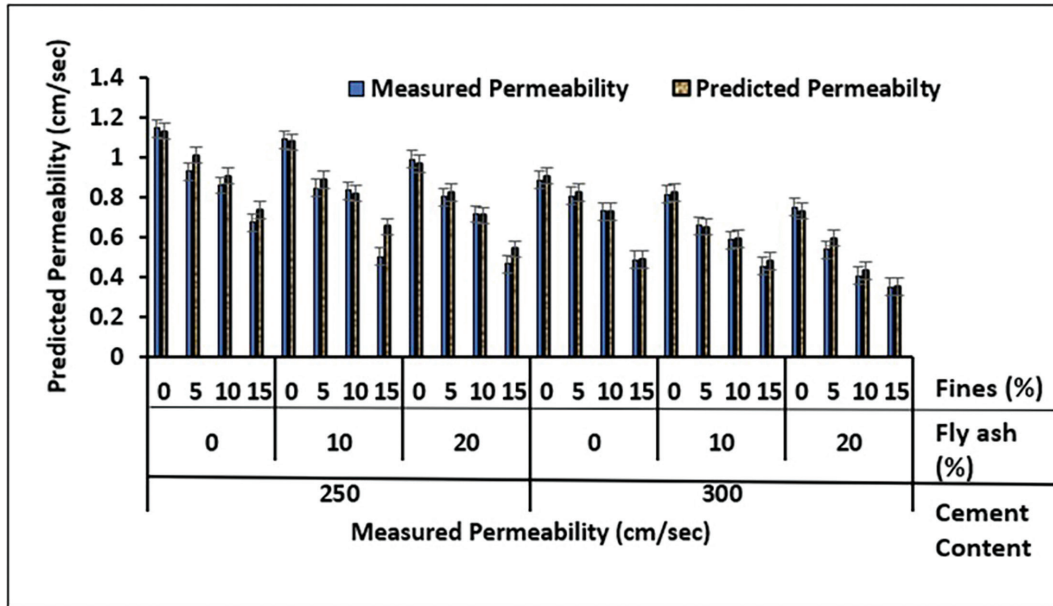


Figure 19: Comparison of permeability (predicated vs experimental) K-T-M for pervious concrete.

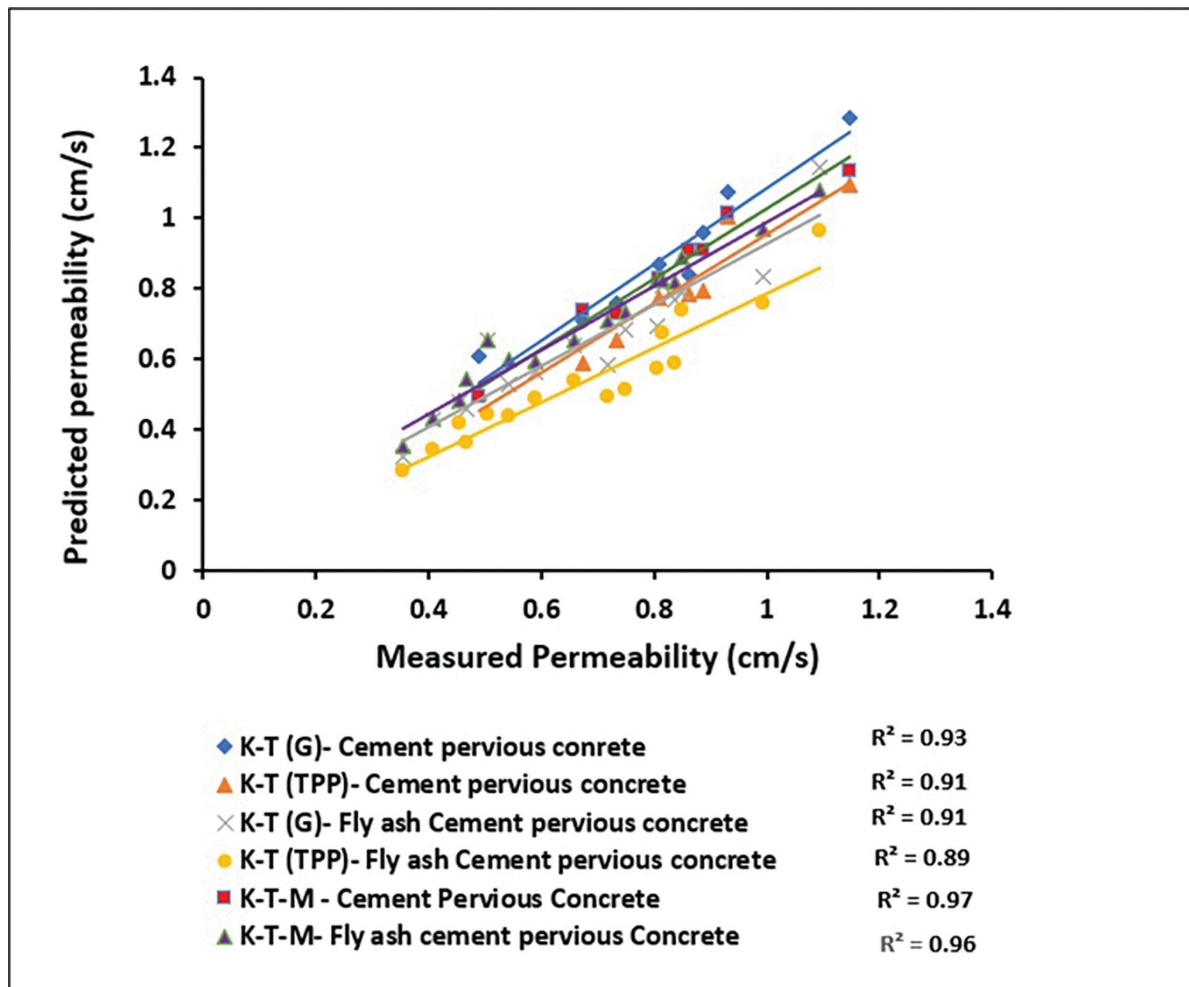


Figure 20: Comparison of experimental and predicted permeability for various models.

recommended to be guided by regional expertise. The American Concrete Pavement Association (ACPA) suggests that a drainage layer beneath concrete pavements should possess a permeability of approximately 107 m/day, equivalent to 1.24 mm/s. Similarly, the aforementioned IRC guideline suggests a lowest level permeability of 300 m/day or higher (0.124 cm/s). It's evident that the advice provided aligns with widely accepted global standards. Furthermore, all the binary blended pervious concrete mixtures met the requirements for void content specified in ACI 522R-10, making them suitable for use as a permeable layer in typical pavement applications in addition to that Residential Driveways, Walkways, Drainage Swales, Road Infrastructure, Bio retention Basins.

5. CONCLUSION

This study deals with the pore structure characteristics of fly ash – cement pervious concrete using image analysis techniques on planar images. The porosity, pore size and its permeability prediction for various fly ash- cement pervious concrete was analyzed. The porosities of pervious concrete obtained from volumetric method and image analysis (area fraction) of planar section is slightly higher than volumetric porosity, which is marginal. The pore size characteristics obtained from two-point correlation and granulometry method were relatively close to each other. Pore size d_{crit} (granulometry) values are slightly higher than d_{TPC} (two-point correlation) method by the same image. Enhancing cement content, incorporating fly ash, and adding sand have the impact of decreasing porosity and pore size in pervious concretes. Permeability of binary blended pervious concrete with and without fines ranges between 1.149 cm/s to 0.354 cm/s. The predicted permeability of the pervious concrete mixtures determined using Katz-Thomson equation and the experimental values of permeability were found to match well. Influence of porosity and pore size on the predicted permeability were found to correlate well. The void contents of all mixes are within the range of void content for pervious concrete specified in ACI 522- R10. Thus, pervious cement fly- ash pervious concrete has the potential for use as permeable lower layers, in a typical pavement.

6. BIBLIOGRAPHY

- [1] AMERICAN CONCRETE INSTITUTE, *ACI 522R-10: report on pervious concrete*, Michigan, ACI, 2010.
- [2] TENNIS, P.D., LEMING, M.L., AKERS, D.J., *Pervious Concrete Pavements: EB302.02*. Maryland, Portland Cement Association, 2004.
- [3] MCCAIN, G.N., DEWOOLKAR, M.M., “Strength and permeability characteristics of porous concrete pavements”, In: *Transportation Research Board 88th Annual Meeting*, Washington DC, 11 March 2009.
- [4] NGUYEN, D.H., SEBAIBI, N., BOUTOUIL, M., *et al.*, “A modified method for the design of pervious concrete mix”, *Construction & Building Materials*, v. 73, pp. 271–282, 2014. doi: <http://dx.doi.org/10.1016/j.conbuildmat.2014.09.088>
- [5] HUANG, B.H., WU, X., SHU, X., *et al.*, “Laboratory evaluation of permeability and strength of polymer – modified pervious concrete”, *Construction & Building Materials*, v. 24, n. 5, pp. 818–823, 2009. doi: <http://dx.doi.org/10.1016/j.conbuildmat.2009.10.025>
- [6] REHDER, B., BANH, K., NEITHALATH, N., “Fracture behavior of pervious concretes: the effects of pore structure and fibers”, *Engineering Fracture Mechanics*, v. 118, pp. 1–16, 2014. doi: <http://dx.doi.org/10.1016/j.engfracmech.2014.01.015>
- [7] AHN, J., JUNG, J., KIM, S., *et al.*, “X-Ray image analysis of porosity of pervious concretes”, *Int. J. of Geomate*, v. 6, n. 1, pp. 796–799, 2014. doi: <http://dx.doi.org/10.21660/2014.11.3249>
- [8] ZHONG, R., WILLE, K., “Linking pore system characteristics to the compressive behavior of pervious concrete”, *Cement and Concrete Composites*, v. 70, pp. 130–138, 2014. doi: <http://dx.doi.org/10.1016/j.cemconcomp.2016.03.016>
- [9] DEO, O., NEITHALATH, N., “Compressive behavior of pervious concretes and a quantification of the influence of random pore structure features”, *Materials Science and Engineering A*, v. 528, n. 1, pp. 402–412, 2010. doi: <http://dx.doi.org/10.1016/j.msea.2010.09.024>
- [10] DEO, O., NEITHALATH, N., “Compressive response of pervious concretes proportioned for desired porosities”, *Construction & Building Materials*, v. 25, n. 11, pp. 4181–4189, 2011. doi: <http://dx.doi.org/10.1016/j.conbuildmat.2011.04.055>
- [11] SUMANASOORIYA, M.S., NEITHALATH, N., “Pore structure features of pervious concretes proportioned for desired porosities and their performance prediction”, *Cement and Concrete Composites*, v. 33, n. 8, pp. 778–787, 2011. doi: <http://dx.doi.org/10.1016/j.cemconcomp.2011.06.002>

- [12] MARTIN III, W., PUTMAN, J., KAYE, N.B., “Using image analysis to measure the porosity distribution of a porous pavement”, *Construction & Building Materials*, v. 48, pp. 210–217, 2013. doi: <http://dx.doi.org/10.1016/j.conbuildmat.2013.06.093>
- [13] SUMANASOORIYA, M.S., NEITHALATH, N., “Stereology- and morphology-based pore structure descriptors of enhanced porosity (Pervious) concretes”, *ACI Materials Journal*, v. 106, n. 5, pp. 429–438, 2009.
- [14] NEITHALATH, N., SUMANASOORIYA, M., DEO, O., “Characterizing pore volume, sizes, and connectivity in pervious concretes for permeability prediction”, *Materials Characterization*, v. 61, n. 8, pp. 802–813, 2010. doi: <http://dx.doi.org/10.1016/j.matchar.2010.05.004>.
- [15] DEBNATH, B., SARKAR, P.P., “Quantification of random pore features of porous concrete mixes prepared with brick aggregate: an application of stereology and mathematical morphology”, *Construction & Building Materials*, v. 294, pp. 123594, 2021. doi: <http://dx.doi.org/10.1016/j.conbuildmat.2021.123594>
- [16] LI, L., YANG, J., YU, X., *et al.*, “Permeability prediction of pervious concrete based on mix proportions and pore characteristics”, *Construction & Building Materials*, v. 395, pp. 132247, 2023. doi: <http://dx.doi.org/10.1016/j.conbuildmat.2023.132247>
- [17] JIANG, Z., PAN, Y., LU, J., *et al.*, “Pore structure characterization of cement paste by different experimental methods and its influence on permeability evaluation”, *Cement and Concrete Research*, v. 159, pp. 106892, 2022. doi: <http://dx.doi.org/10.1016/j.cemconres.2022.106892>
- [18] GUAN, X., MIAO, L., LU, R., *et al.*, “Experimental study on Katz-Thompson model for concrete materials and determination of K-T constant”, *Magazine of Concrete Research*, v. 71, n. 4, pp. 207–216, 2019. doi: <http://dx.doi.org/10.1680/jmacr.17.00374>
- [19] CHEN, J., YU, S., HUANG, W., *et al.*, “Two-dimensional microstructure-based model for evaluating the permeability coefficient of heterogeneous”, *Materials (Basel)*, v. 16, n. 17, pp. 5892, 2023. doi: <http://dx.doi.org/10.3390/ma16175892>. PubMed PMID: 37687585
- [20] HUANG, J., ZHANG, Y., SUN, Y., *et al.*, “Evaluation of pore size distribution and permeability reduction behavior in pervious concrete”, *Construction & Building Materials*, v. 290, pp. 123228, 2021. doi: <http://dx.doi.org/10.1016/j.conbuildmat.2021.123228>
- [21] WANG, Q., ZHANG, G., TONG, Y., *et al.*, “Prediction on permeability of engineered cementitious composites”, *Crystals*, v. 11, n. 5, pp. 526, 2021. doi: <http://dx.doi.org/10.3390/cryst11050526>
- [22] DEBNATH, B., SARKAR, P., “Permeability prediction and pore structure feature of pervious concrete using brick as aggregate”, *Construction & Building Materials*, v. 213, pp. 643–651, 2019. doi: <http://dx.doi.org/10.1016/j.conbuildmat.2019.04.099>
- [23] LIU, R., CHI, Y., CHEN, S., *et al.*, “Influence of pore structure characteristics on the mechanical and durability behavior of pervious concrete material based on image analysis”, *International Journal of Concrete Structures and Materials*, v. 14, n. 1, pp. 29, 2020. doi: <http://dx.doi.org/10.1186/s40069-020-00404-1>
- [24] WANG, Z., ZOU, D., LIU, T., *et al.*, “A novel method to predict the mesostructure and performance of pervious concrete”, *Construction & Building Materials*, v. 263, pp. 120117, 2020. doi: <http://dx.doi.org/10.1016/j.conbuildmat.2020.120117>
- [25] NEITHALATH, N., WEISS, J., OLEK, J., “Characterizing Enhanced Porosity Concrete using electrical impedance to predict acoustic and hydraulic performance”, *Cement and Concrete Research*, v. 36, n. 11, pp. 2074–2085, 2006. doi: <http://dx.doi.org/10.1016/j.cemconres.2006.09.001>
- [26] KATZ, A.J., THOMPSON, A.H., “Quantitative prediction of permeability in porous rock”, *Physical Review B: Condensed Matter*, v. 34, n. 11, pp. 8179–8181, 1986. doi: <http://dx.doi.org/10.1103/PhysRevB.34.8179>. PubMed PMID: 9939522.
- [27] SCHWARTZ, L.M., MARTYS, N., BENTZ, D.P., *et al.*, “Cross property relations and permeability estimation in model porous media”, *Physical Review E*, v. 48, n. 6, pp. 4584–4591, 1993. doi: <http://dx.doi.org/10.1103/PhysRevE.48.4584>. PubMed PMID: 9961139
- [28] ISCAN, G., KOK, M.V., “Porosity and permeability determinations in sandstone and limestone rocks using thin section analysis approach”, *Energy Sources. Part A, Recovery, Utilization, and Environmental Effects*, v. 31, n. 7, pp. 568–575, 2009. doi: <http://dx.doi.org/10.1080/15567030802463984>
- [29] CHRISTENSEN, B.J., MASON, T.O., JENNINGS, H.M., “Comparison of measured and calculated permeability for cement pastes”, *Cement and Concrete Research*, v. 26, n. 9, pp. 1325–1334, 1996. doi: [http://dx.doi.org/10.1016/0008-8846\(96\)00130-5](http://dx.doi.org/10.1016/0008-8846(96)00130-5)

- [30] NOKKEN, M.R., HOOTON, R.D., “Using pore parameters to estimate permeability or conductivity of concrete”, *Materials and Structures*, v. 41, n. 1, pp. 1–16, 2006. doi: <http://dx.doi.org/10.1617/s11527-006-9212-y>
- [31] HU, J., STROEVEN, P., “Local porosity analysis of pore structure in cement paste”, *Cement and Concrete Research*, v. 35, n. 2, pp. 233–242, 2005. doi: <http://dx.doi.org/10.1016/j.cemconres.2004.06.018>
- [32] COSTER, M., CHERMANT, J.L., “Image analysis and mathematical morphology for civil engineering materials”, *Cement and Concrete Research*, v. 23, n. 2-3, pp. 133–151, 2001. doi: [http://dx.doi.org/10.1016/S0958-9465\(00\)00058-5](http://dx.doi.org/10.1016/S0958-9465(00)00058-5)